



Formation of Ni chains induced by self-generated magnetic field

Chunhong Gong, Juntao Tian, Tao Zhao, Zhishen Wu, Zhijun Zhang*

Key Laboratory of Special Functional Materials of Ministry of Education, Henan University, Kaifeng 475001, PR China

ARTICLE INFO

Article history:

Received 15 September 2007
Received in revised form 28 March 2008
Accepted 17 April 2008
Available online 24 April 2008

Keywords:

A. Metals
B. Chemical synthesis
C. Electron microscopy
D. Magnetic properties

ABSTRACT

Ultrafine chain-like Ni assemblies with a length of about 5 μm were successfully prepared by the reduction of Ni salts with hydrazine hydrate under normal pressure in the absence of any inorganic or organic templates. The resulting Ni chains were characterized by means of X-ray diffraction (XRD) and scanning electron microscopy (SEM). Moreover, the growth process of the Ni chains was investigated for the first time, using transmission electron microscopy (TEM) and XRD as well, which is valuable to study the self-assembly mechanism of magnetic nanocrystallites. Results indicated that the novel chain-like Ni assemblies were integrated from Ni microspheres with a diameter of about 250 nm. Magnetic hysteresis measurement revealed that the Ni chains showed ferromagnetic behavior with a saturation magnetization of 15.07 emu/g and a coercivity of 115.1 Oe at room temperature. It was supposed that the self-generated magnetic field could induce the formation of the Ni chains.

© 2008 Elsevier Ltd. All rights reserved.

1. Introduction

Recently, nanosized metal magnetic materials have been extensively highlighted because of their expected intriguing properties when compared with their bulk stuffs [1–6]. In particular, anisotropic one-dimensional (1D) magnetic nanoscale materials have attracted much attention because of their potential applications in magnetic sensors, memory devices, catalysts and galvanomagnetic materials [7–9]. Taking nickel as an example, various methods have been developed for the synthesis of nanosized nickel with different shapes, and the morphology control of Ni has been an active research theme [10–14]. Through those research experiments, hollow microspheres of nickel [13,14], triagonal nickel nanoparticles [15], and flower shaped nickel nanocrystals [16], together with different 1D nickel nanostructures such as single-crystal Ni nanobelts [17] and polycrystalline Ni wires [18] have been successfully fabricated using various methods [19,20].

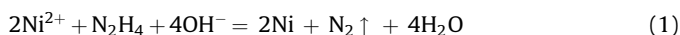
The fabrication of Ni nanowires mainly depends on a template technique that involves electrochemical deposition or metal organic chemical vapor deposition (CVD) of metals into the nanopores of template materials [18,21–26] such as anodic aluminum oxide (AAO) film [21,22], carbon nanotubes [23] and porous silicon (PS) [12,26]. The template technique has been successfully used, as one of versatile approaches, in the preparation of the arrays of some magnetic nanomaterials such as Fe, Co, Ni and alloy nanowires [18]. However, the template-based

synthetic routes are unfavorable in terms of the complicated synthetic procedures with respect to the purification process (removal of the templates) of the final products. Therefore, it is imperative to develop template-free methods for the fabrication of 1D magnetic nanomaterials. The magnetic field-directed assembly used for the fabrication of various 1D metal magnetic nanostructures gives one of the examples of the template-free methods [27–32]. As a kind of permanent magnetic materials, metallic nickel has inherent magnetism. Thus we suppose that magnetic Ni particles could magnetize those particulates nearby via dipolar interaction, leading to the 1D self-assembly of the magnetic nanocrystallites even in the absence of external magnetic fields. To testify this point of view, in the present work we prepared ultrafine Ni chains via a very simple reduction process—the reduction of nickel chloride by hydrazine hydrate under normal pressure and in the absence of any morphology-controlling media such as exterior magnetic field, template materials, and surfactants or passivating materials, aiming at simplifying the synthesis procedures and avoiding introduction of impurities into the final products. The resulting Ni chains were characterized by means of SEM and XRD, and their magnetic properties were measured as well. The formation process of the Ni chains in the presence of the self-generated magnetic field was also analyzed using TEM and XRD. This article deals with the relevant research results, and hopefully, it would help to acquire new insights into the growth and self-assembly mechanisms of nickel nanocrystallites and design of a new general method for the preparation of other magnetic metal nanostructures with a broad range of well-defined and controllable morphologies, so as to fully exploit their peculiar properties and unique applications.

* Corresponding author. Tel.: +86 378 3881358; fax: +86 378 3881358.
E-mail address: jwzhang@henu.edu.cn (Z. Zhang).

2. Experimental

All the reagents are analytical grade, and used without further purification. In a typical process, firstly, 0.118 g of nickel chloride ($\text{NiCl}_2 \cdot 6\text{H}_2\text{O}$, Tianjin Kermel Chemical Co., Ltd., China) was dissolved into 50 ml of ethylene glycol (EG, Tianjin Kermel Chemical Co., Ltd., China) to give a green transparent solution, allowing the homogeneous dispersion of Ni^{2+} . Then 1 ml of hydrazine hydrate solution ($\text{N}_2\text{H}_4 \cdot \text{H}_2\text{O}$, concentration 80 wt%, Tianjin Kermel Chemical Co., Ltd., China) was added dropwise into the reseda solution under continuous stirring, allowing the generation of a lavender solution within several minutes. Thirdly, 2 ml of 1 M NaOH (Tianjin Deen Chemical Co., Ltd., China) solution was added dropwise into the lavender solution, allowing the generation of a sky-blue solution in several minutes. The sky-blue solution was then, in the absence of stirring, heated to 60°C and held there for a few minutes, to allow the appearance of black floccules and very quick change to black of the solution color. Several minutes later, the solution became clear and colorless, while the desired black fluffy solid product was floating atop the reaction solution, indicating the formation of metallic Ni. The chemical reaction for the synthesis can be expressed as:



where Ni^{2+} ions were reduced into zero-valenced Ni by N_2H_4 and the nitrogen gas produced could help to protect the nascent nickel nanocrystallites from oxidation. In order to demonstrate the effect of stirring on the formation of Ni products, similar experiment was performed under the same conditions but the solution was stirred mechanically. At the end of the reaction, the products were collected with the assistance of magnetic separation and washed with alcohol for several times to remove the ions and other materials possibly remaining in the final product, and finally dried in a vacuum at 40°C for 24 h. The obtained products were characterized using a Philips X' Pert Pro X-ray diffractometer (XRD, $\text{Cu K}\alpha$ radiation, $\lambda = 0.15418 \text{ nm}$) and a JEOL JSM-5600LV scanning electron microscope (SEM, acceleration voltage 20 kV). The magnetic hysteresis loop of the product at room temperature was measured using a sample-vibrating magnetometer (VSM, Lake Shore 7300, USA). A JEOL JEM-2010 transmission electron

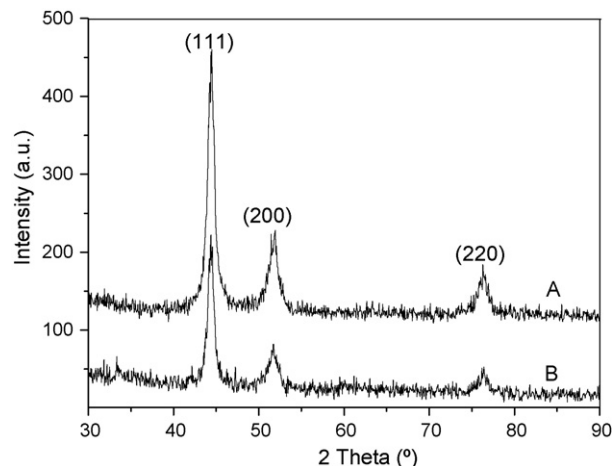


Fig. 1. XRD patterns for the final Ni samples obtained at the end of the reaction under stillness condition (A) and stirring condition (B).

microscope (TEM, accelerating voltage 200 kV) was performed to record the microscopic images and selected area electron diffraction (SAED) patterns of the samples obtained at different reaction durations, aiming at revealing the details about the growth process of the ultrafine Ni chains. The samples for the TEM analysis were collected via centrifuging separation. After being washed and dispersed with alcohol in the presence of ultrasonic stirring, a few drops of the dispersed alcohol solution were introduced onto a carbon-coated copper grid and allowed to evaporate in air at room temperature. Then the samples were ready for the TEM analysis.

3. Results and discussion

Fig. 1 depicts the XRD patterns of two typical Ni samples prepared from the reaction systems kept in stillness (Fig. 1A) and under stirred condition (Fig. 1B). Three characteristic peaks for Ni ($2\theta = 44.5^\circ$, 51.8° , and 76.4°), corresponding to Miller indices (1 1 1), (2 0 0), and (2 2 0), were observed for both samples, indicating that they were both composed of pure face-centered

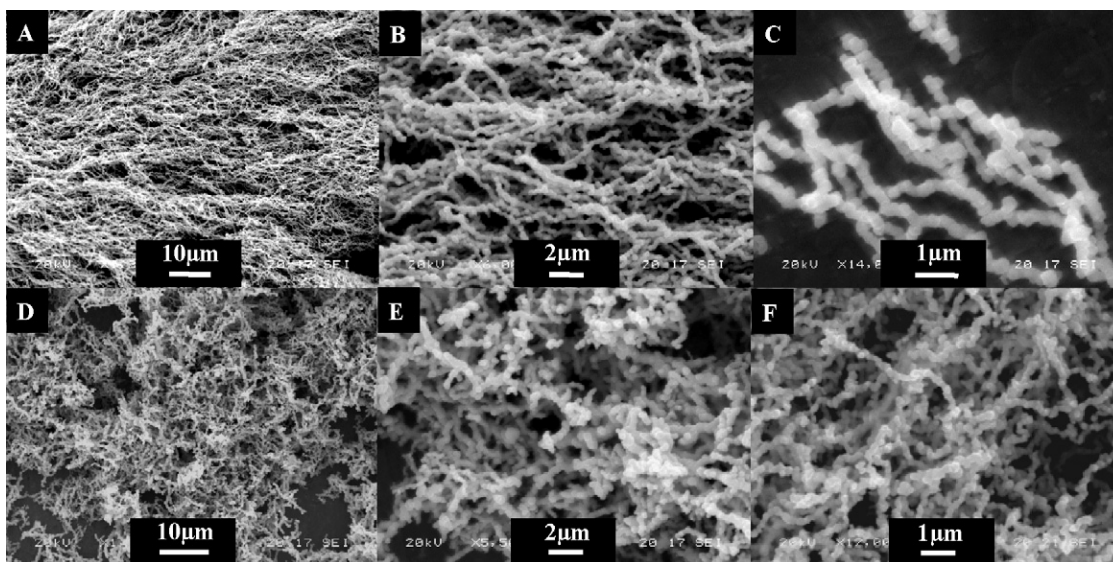


Fig. 2. SEM images of the final samples formed under different reaction conditions: (A) the overall morphology of the ultrafine Ni chains formed under stillness condition; (B) and (C) the magnified SEM images of the Ni chains; (D) and (E) the SEM images of the samples obtained under stirring condition; (F) the SEM image of the Ni chains treated by ultrasonic vibration for 10 min.

cubic (fcc) Ni (PDF standard cards, JCPDS 01–1260, space group $Fm\bar{3}m$) and did not contain impurities [28]. Though nickel is easily oxidized, peaks due to its oxide were not observed, which might be due to the fact that the reaction was carried out at appropriate pH, temperature and hydrazine concentration, and inactive N_2 was produced and acted as a kind of protective atmosphere.

The SEM morphologies of the Ni samples obtained under stillness and stirred condition are shown in Fig. 2, where Fig. 2A is the overall morphology of the chain-like Ni sample. It is seen that all the Ni samples exhibit a squiggly chain-like configuration. The magnified SEM image shown in Fig. 2B indicates that all of the Ni chains are made up of spherical-like particles with a diameter of

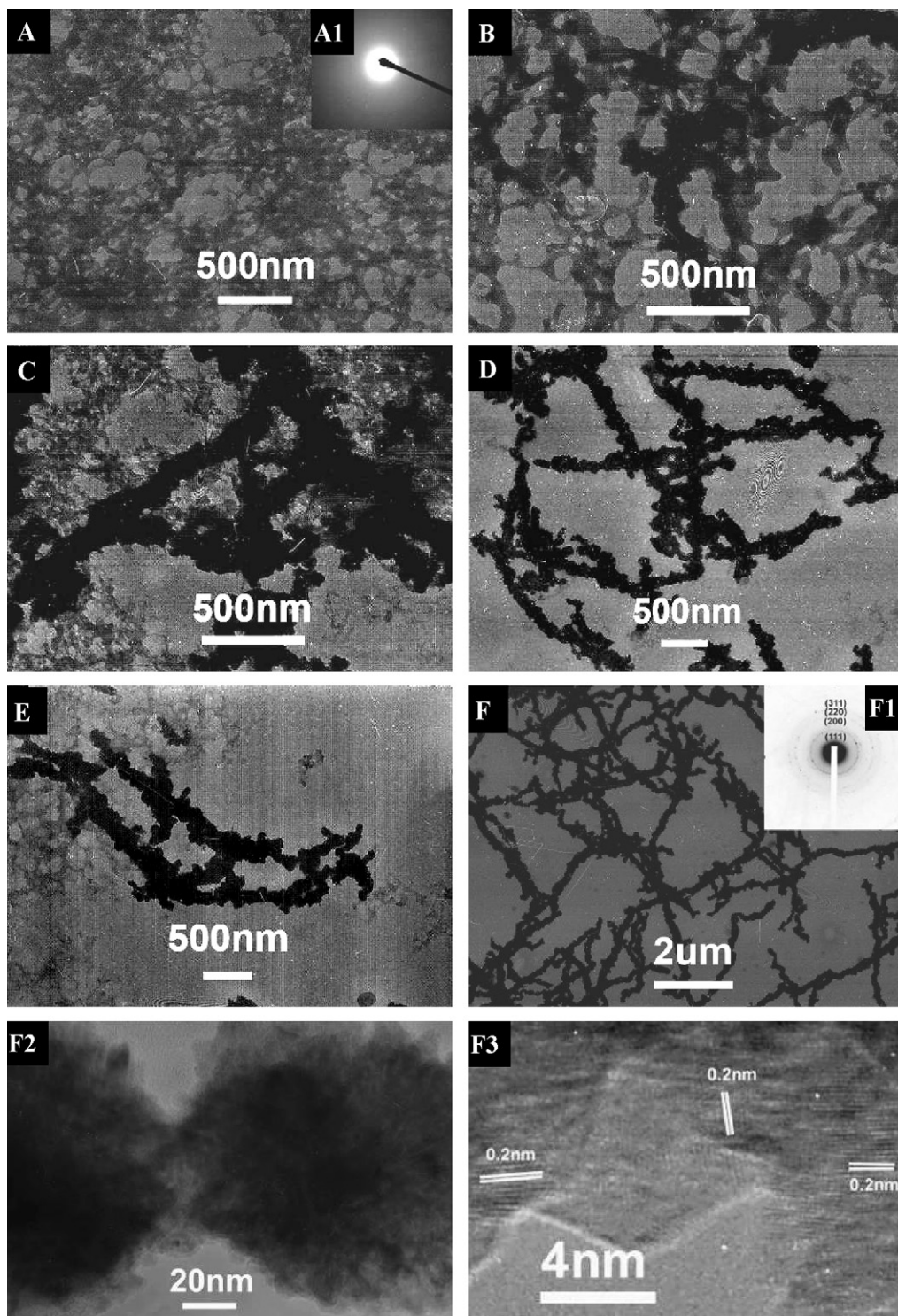


Fig. 3. TEM images of the as-prepared samples taken out at different reaction time: (A) 0 s, (B) 10 s, (C) 20 s, (D) 1 min, (E) 1.5 min, and (F) 2 min. (A1) the electron diffraction (ED) pattern of sample A, (F1) the electron diffraction (ED) pattern obtain from the edge of a single chain, (F2) the magnified image of the interlinks between the spherical particles of a chain, and (F3) the high-resolution (HRTEM) image from the joint zone.

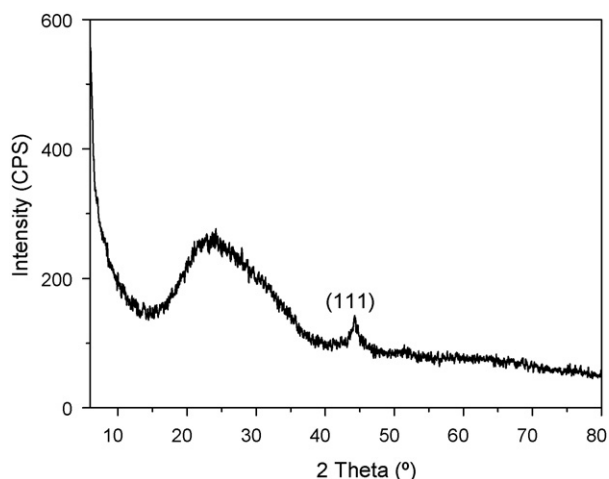


Fig. 4. XRD pattern of the product obtained at a reaction time of 20 s.

about 250 nm, and the particles are closely contacted with each other to form squiggly chains with a length of about 5 μm . The high-magnification images of several Ni chains shown in Fig. 2C reveal a clear and well-defined chain structure consisting of Ni microparticles with quite smooth surface. Whereas, the products obtained under stirred solution seem to be scrappy and exhibit dendrite-like configuration (Fig. 2D and E). Moreover, to investigate the strength of the chains, the final chain-like products (Fig. 2A) were ultrasonically vibrated at a power of 100 W (KQ-218, Kunshan Ultrasonic Instruments Co., Ltd., China) for over 10 min and then were observed with SEM. Obviously, the morphologies of the Ni chains kept almost unchanged after ultrasonic vibration (Fig. 2F), implying that the Ni particles were inclined to grow together rather than merely aggregate one another.

The formation of the Ni chains should be dependent on the intrinsic growth behavior of the Ni crystal and the external experimental conditions such as reactant concentration, temperature, type of surfactants etc. Thus, the mechanism for the growth of one-dimensional Ni chains is very complicated and has yet not been well revealed [32]. Fu and co-workers reported the preparation of chain-like CoNi alloy assemblies by a surfactant-assisted hydrothermal synthetic route and assumed that the surfactants cetyltrimethylammonium bromide (CTAB) or cetyltrimethylammonium chloride (CTAC) could act as a template, which

led to a chain-like structure [33]. Since the present reaction could be easily conducted in an open system, a series of samples were collected at different reaction stages and analyzed by TEM, aiming at acquiring more insights into the formation process of the Ni chains. Because the reaction progressed very quickly (Once the black floccules appeared in the solution, the reaction would be finished in several minutes), the sampling process had to be timely and expeditious. Namely, once the target samples were taken out from the reaction solution, they were immediately put into liquid nitrogen so as to ensure timely interruption of the reaction. When the black floccules appeared, the first sample was extracted out; then five more samples were extracted at an interval of 10 s, 20 s, 1 min, 1.5 min, and 2 min, respectively. The corresponding TEM images of the totally six samples are labeled as A–F, respectively, in Fig. 3.

At the initial reaction process, only floccules appeared in the reactant solution and the floccules in this case were amorphous (see Fig. 3A and A1 insert). With the proceeding of the reaction for different durations, some short chain-like products emerged quickly (see Fig. 3B and C). The XRD pattern of sample C (see Fig. 4) shows a broad amorphous peak centered at $2\theta = 24^\circ$ and a small diffraction peak at $2\theta = 44.5^\circ$, which can be assigned to Ni (1 1 1). In combination with the TEM image of sample C (see Fig. 3C), it could be concluded that, at a reaction duration of 20 s, the corresponding products were composed of amorphous flocculent compound and crystalline nickel chains. With further increase in the reaction duration up to 1 min and 1.5 min, more and more chains with larger lengths were produced, and meanwhile the proportion of the floccules decreased (see Fig. 3D and E). As the reaction duration was extended to 2 min, only chain-like product was obtained (see Fig. 3F). The SAED pattern of a single chain of sample F is displayed in Fig. 3F1, where the four fringe patterns can be indexed as (1 1 1), (2 0 0), (2 2 0), (3 1 1) of pure face-centered cubic (fcc) nickel, indicating that the nickel chains in this case had polycrystalline structure. Similarly, as shown in Fig. 3F2, the magnified image at the joint between the spherical particles of a chain indicated that the Ni chains consisted of spherical particles with a size of 100–200 nm. A high-resolution TEM image from the joint of two spherical particles is shown in Fig. 3F3, where the (1 1 1) planes, with an inter-planar spacing of about 0.2 nm, are marked with a series of parallel lines. It is seen that the (1 1 1) planes have different orientations in different domains, which is one of the characteristics of polycrystalline structures. Combining Fig. 3F2 and Fig. 3F3, it could be inferred that the spherical Ni

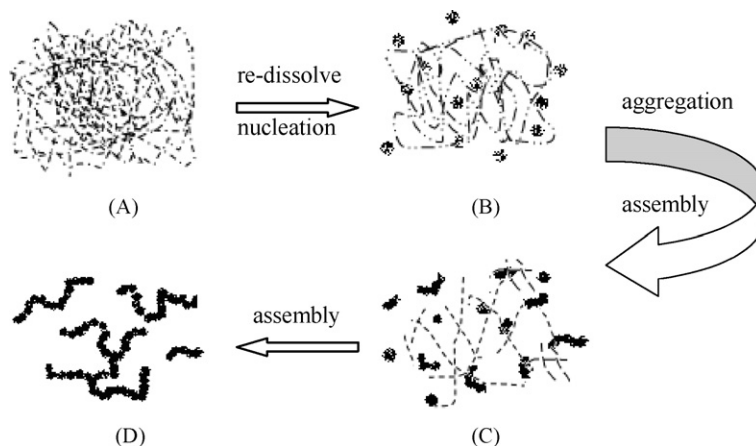


Fig. 5. Schematic illustration of the formation of the ultrafine Ni chains assemblies: (A) the formation of the intermediate amorphous-phase floccules; (B) the re-dissolving of the intermediate phase and the nucleation; (C) the aggregation of the nickel primary nuclei and the generation of the short Ni chain-like assemblies; (D) longer Ni chains formed.

particles did not merely attract one another but did grow together; in consistency with the corresponding SEM analytical results (see Fig. 2F).

Based on the above-mentioned experimental results, a schematic illustration of the formation mechanism of the as-synthesized chain-like Ni assemblies is shown in Fig. 5, where the Ni (II) species are involved in an equilibrium between the solution and the unreduced intermediate phase. Initially, an unknown intermediate phase—amorphous floccules were generated in the reactant solution at the beginning of the reaction, which might act as Ni source materials and could sharply decrease the concentration of free Ni²⁺ in the solution, resulting in a relatively slow rate of generation of Ni atoms (see Figs. 3A and 5A). Then the intermediate solid phase could be re-dissolved with the increase of the reaction time, and two-valence Ni, during rising of its concentration above the saturation concentration, was reduced to zero-valence Ni [34,35], accompanied by the collision of initially reduced metal atoms and their nucleating (see Fig. 5B). Along with the reaction, the small Ni primary nuclei acted as seeds to allow more metal atoms to be reduced and absorbed on the nuclei, and the reduced Ni atoms were inclined to aggregate into larger particles for the sake of decreasing surface energy. As a kind of permanent magnetic materials, each nickel particle with a big enough size has an inherent self-generated magnetic field. Driven by the self-generated magnetic field, the Ni particles would prefer aggregating along the magnetic force lines. Consequently, the desired ultrafine Ni chain-like assemblies would be generated at properly extended reaction durations (see Figs. 3A–E and 5C). As time prolonged, these chains transformed into longer ones and meanwhile the proportion of the amorphous floccules decreased until vanished (see Fig. 3F and 5D). However, since the self-generated magnetic field of the Ni particle is very weak, the disturbing forces caused by the uneven temperature in the solution and Brownian motion should not be neglected. Actually, the formation of the final squiggly chained target products in the present research was a compromise between the oriented magnetic force and the random disturbing. This process had better be handled only when the magnetization of the particles in the suspension did not fluctuate during the magnetic interaction. In other words, when the reaction system was stirred, the oriented growth of the magnetic nanocrystallites would be destroyed partially and the particles could contact with each other in any directions, resulting in branched and short dendrite-like configuration.

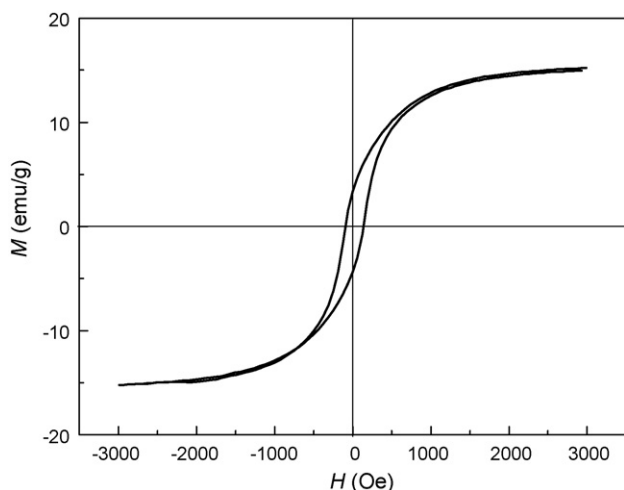


Fig. 6. The hysteresis loop of the final chain-like Ni samples obtained at the end of the reaction measured at room temperature.

The magnetic properties of the chain-like Ni products were investigated using a sample-vibrating magnetometer. Plot of magnetization vs. applied magnetic field for the chain-like Ni samples obtained at the end of the reaction is shown in Fig. 6, where the hysteresis loop shows obvious ferromagnetic characteristics at room temperature. The specific saturation magnetization (M_s) and the coercivity (H_c) values for the Ni chains were calculated to be 15.07 emu/g and 115.1 Oe, respectively. Namely, the as-prepared chain-like Ni samples obtained in the presence of self-generated magnetic field had lower saturation magnetization and higher coercivity than the bulk Ni sample at room temperature ($M_s = 54\text{--}55$ emu/g, $H_c = 100$ Oe) [36,37].

It is well known that the crystallite size, structures and shapes of magnetic materials have effects on the magnetic properties of the products [32,38–40]. Generally, the M_s for nanoscale magnetic materials is lower than that for bulk material because the spin disorder on the surface significantly reduces the total magnetic moment [10], and the shape of the hysteresis loop is strongly affected not only by the specific surface area of the particles but also by the magnetic anisotropy [33], including magnetocrystalline anisotropy, shape anisotropy, stress anisotropy, induced anisotropy and exchange anisotropy [41]. This could be cited to well explain the decrease of M_s for the Ni nanostructures in the present work. Namely, the synthesized representative chain-like Ni assemblies had an average aspect ratio of about 20, implying obvious shape anisotropy and hence increased coercivity as well. Therefore, the higher coercivity of the as-prepared chain-like Ni samples as compared with bulk Ni sample might be attributed to their special nanostructure characterized by reduced size and shape anisotropy, which could prevent them from oriental magnetizing other than along their easy magnetic axes, leading to a higher coercivity [10,29].

4. Conclusions

In summary, a novel and facile route for producing ultrafine Ni chains via a mild reduction process in the absence of any exterior morphology-controlling techniques and/or devices has been reported. The present method could be superior to other types of synthetic routes in terms of the mild reaction conditions such as normal pressure and lowered temperature, and might be extended to the synthesis of other types of magnetic chains. The self-assembly mechanisms of the Ni nanocrystallites induced by self-generated magnetic field were investigated for the first time, which could help to better understand the formation process of the chain-like Ni assemblies and to improve the efficiencies of various devices based on single particles or their composites as well [33,42]. It was found that in the absence of exterior magnetic field, the one-dimensional self-assembly of nickel nanocrystallites could be induced by their magnetic attraction. The morphologies and microstructures of the resulting chain-like ultrafine Ni particles were highly dependent on the reaction duration. The chain-like Ni nanostructures showed ferromagnetic characteristics and had saturation magnetization (M_s) and coercivity (H_c) of 15.07 emu/g and 115.1 Oe, respectively, showing lower saturation magnetization and higher coercivity than bulk Ni sample at room temperature.

Acknowledgments

The authors have benefited a lot from the helpful discussion with Prof. Zhen-sheng Jin and Si-xin Wu in our laboratory. The financial support from the Ministry of Science and Technology of China (Grant No. 2007CB607606, in the name of “973” Plan) is acknowledged. Special thanks are due to Dr. Lai-gui Yu for help in manuscript preparation.

References

- [1] S. Sun, H. Zeng, *J. Am. Chem. Soc.* 124 (2002) 8204.
- [2] C.C. Chen, A.B. Herhold, C.S. Johnson, A.P. Alivisatos, *Science* 276 (1997) 398.
- [3] V.F. Puentes, K.M. Krishnan, A.P. Alivisatos, *Science* 291 (2001) 2115.
- [4] D.J. Milliron, S.M. Hughes, Y. Cui, L. Manna, J.B. Li, L.W. Wang, A.P. Alivisatos, *Nature* 430 (2004) 190.
- [5] Y.D. Yin, R.M. Rioux, C.K. Erdonmez, S. Hughes, G.A. Somorjai, A.P. Alivisatos, *Science* 304 (2004) 711.
- [6] X.M. Liu, S.Y. Fu, C.J. Huang, *J. Magn. Magn. Mater.* 281 (2004) 234.
- [7] S. Pignard, G. Goglio, A. Radulescu, L. Piroux, S. Dubois, A. Declémy, J.L. Duvail, *J. Appl. Phys.* 87 (2000) 824.
- [8] L. Sun, P.C. Searson, C.L. Chien, *Appl. Phys. Lett.* 79 (2001) 4429.
- [9] C. Beeli, *Nanostruct. Mater.* 11 (1999) 697.
- [10] X.M. Liu, S.Y. Fu, *J. Cryst. Growth* 306 (2007) 428.
- [11] Y. Hou, H. Kondoh, T. Ohta, S. Gao, *Appl. Surf. Sci.* 241 (2005) 218.
- [12] P. Granitzer, K. Rumpf, P. Pölt, A. Reichmann, M. Hofmayer, H. Krenn, *J. Magn. Magn. Mater.* 316 (2007) 302.
- [13] Q. Liu, H.J. Liu, M. Han, J.M. Zhu, Y.Y. Liang, Z. Xu, Y. Song, *Adv. Mater.* 17 (2005) 1995.
- [14] M. Ning, H.F. Zhu, Y.S. Jia, H. Niu, M.Z. Wu, Q.W. Chen, *J. Mater. Sci.* 40 (2005) 4411.
- [15] J.S. Bradley, B. Tesche, W. Busser, M. Maase, M.T. Reetz, *J. Am. Chem. Soc.* 122 (2000) 4631.
- [16] X.M. Ni, Q.B. Zhao, H.G. Zheng, B.B. Li, J.M. Song, D.G. Zhang, X.J. Zhang, *Eur. J. Inorg. Chem.* (2005) 4788.
- [17] Z.P. Liu, S. Li, Y. Yang, S. Peng, Z.K. Hu, Y.T. Qian, *Adv. Mater.* 15 (2003) 1946.
- [18] H.Q. Cao, Z. Xu, D. Sheng, J.M. Hong, H. Sang, Y.W. Du, *J. Mater. Chem.* 11 (2001) 958.
- [19] N. Cordente, M. Respaud, F. Senocq, M. Casanove, C. Amiens, B. Chaudret, *Nano Lett.* 1 (2001) 565.
- [20] J.C. Bao, C.Y. Tie, Z. Xu, Q.F. Zhou, D. Shen, Q. Ma, *Adv. Mater.* 13 (2001) 1631.
- [21] S.G. Yang, H. Zhu, D.L. Yu, Z.Q. Jin, S.L. Tang, Y.W. Du, *J. Magn. Magn. Mater.* 222 (2000) 97.
- [22] K. Nielsch, R.B. Wehrspohn, J. Barthel, J. Kirschner, S.F. Fischer, H. Kronmüller, T. Schweinböck, D. Weiss, U. Gösele, *J. Magn. Magn. Mater.* 249 (2002) 234.
- [23] B.K. Pradhan, T. Kyotani, A. Tomita, *Chem. Commun.* 14 (1999) 1317.
- [24] H. Masuda, K. Fukuda, *Science* 268 (1995) 1466.
- [25] S. Kato, H. Shinagawa, H. Okada, G. Kido, K. Mitsuhashi, *Sci. Technol. Adv. Mater.* 6 (2005) 341.
- [26] P. Granitzer, K. Rumpf, P. Pölt, A. Reichmann, H. Krenn, *J. Magn. Magn. Mater.* 310 (2007) 838.
- [27] H.L. Niu, Q.W. Chen, H.F. Zhu, Y.S. Lin, X. Zhang, *J. Mater. Chem.* 13 (2003) 1803.
- [28] H.L. Niu, Q.W. Chen, M. Ning, Y.S. Jia, X.J. Wang, *J. Phys. Chem. B* 108 (2004) 3996.
- [29] J. Wang, Q.W. Chen, C. Zeng, B.Y. Hou, *Adv. Mater.* 16 (2004) 137.
- [30] L.X. Zhang, J. Luo, Q.W. Chen, *J. Phys.: Condens. Matter* 17 (2005) 5095.
- [31] G.J. Cheng, D. Romero, G.T. Fraser, A.R.H. Walker, *Langmuir* 21 (2005) 12055.
- [32] J. Wang, Q.W. Chen, S. Che, *J. Magn. Magn. Mater.* 280 (2004) 281.
- [33] L.P. Zhu, H.M. Xiao, S.Y. Fu, *Eur. J. Inorg. Chem.* (2007) 3947.
- [34] C.L. Jiang, G.F. Zou, W.Q. Zhang, W.C. Yu, Y.T. Qian, *Mater. Lett.* 60 (2006) 2319.
- [35] X.M. Liu, S.Y. Fu, C.J. Huang, *Mater. Lett.* 59 (2005) 3791.
- [36] J.H. Hwang, V.P. Dravid, M.H. Teng, J.J. Host, B.R. Elliott, D.L. Johnson, T.O. Mason, *J. Mater. Res.* 12 (1997) 1076.
- [37] Y.W. Du, M.X. Xu, J. Wu, Y.B. Shi, H.X. Lu, *J. Appl. Phys.* 70 (1991) 5903.
- [38] K.V.P.M. Shafi, A. Gedanken, R. Prozorov, J. Balogh, *Chem. Mater.* 10 (1998) 3445.
- [39] P. Fulmer, M.M. Raja, A. Manthiram, *Chem. Mater.* 13 (2001) 2160.
- [40] H.T. Zhang, G. Wu, X.H. Chen, X.G. Qiu, *Mater. Res. Bull.* 41 (2006) 495.
- [41] L.L.P. Diandra, D.R. Reuben, *Chem. Mater.* 8 (1996) 1770.
- [42] Z.Y. Tang, N.A. Kotov, *Adv. Mater.* 17 (2005) 951.